Tryptophan−Heme π-Electrostatic Interactions in Cytochrome *f* of Oxygenic Photosynthesis[†]

Mikhail V. Ponamarev,[‡] Beatrix G. Schlarb,[§] Christopher J. Howe,[§] Christopher J. Carrell,[‡] Janet L. Smith,[‡] Derek S. Bendall,[§] and William A. Cramer*,[‡]

Department of Biological Sciences, Purdue University, West Lafayette, Indiana 47907, and Department of Biochemistry and Centre for Molecular Recognition, University of Cambridge, Tennis Court Road, The Downing Site, Cambridge CB2 1QW, U.K.

Received December 17, 1999; Revised Manuscript Received March 9, 2000

ABSTRACT: Cytochrome *f* of oxygenic photosynthesis has an unprecedented structure, including the N-terminus being a heme ligand. The adjacent N-terminal heme-shielding domain is enriched in aromatic amino acids. The atomic structures of the chloroplast and cyanobacterial cytochromes *f* were compared to explain spectral and redox differences between them. The conserved aromatic side chain in the N-terminal heme-shielding peptide at position 4, Phe and Tyr in plants and algae, respectively, and Trp in cyanobacteria, is in contact with the heme. Mutagenesis of cytochrome *f* from the eukaryotic green alga *Chlamydomonas reinhardtii* showed that a Phe4 → Trp substitution in the N-terminal domain was unique in causing a red shift of 1 and 2 nm in the cytochrome Soret (γ) and Q (α) visible absorption bands, respectively. The resulting α band peak at 556 nm is characteristic of the cyanobacterial cytochrome. Conversely, a Trp4 → Phe mutation in the expressed cytochrome from the cyanobacterium *Phormidium laminosum* caused a blue shift to the 554 nm α band peak diagnostic of the chloroplast cytochrome. Residue 4 was found to be the sole determinant of this 60 cm^{-1} spectral shift, and of approximately one-half of the 70 mV redox potential difference between cytochrome *f* of *P. laminosum* and *C. reinhardtii* (E_{m7} = 297 and 370 mV, respectively). The proximity of Trp-4 to the heme implies that the spectral and redox potential shifts arise through differential interaction of its σ- or π-electrostatic potential with the heme ring and of the π-potential with the heme Fe orbitals, respectively. The dependence of the visible spectrum and redox potential of cytochrome *f* on the identity of aromatic residue 4 provides an example of the use of the relatively sharp cytochrome spectrum as a "spectral fingerprint", and of the novel structural connection between the heme and a single nonliganding residue.

The optical spectra and oxidation−reduction potentials of redox proteins depend on details of the protein structure in a manner that is not understood (*1*). It has not been possible to attribute shifts in spectra or redox potential in any respiratory or photosynthetic cytochrome to specific interactions of the heme with a single amino acid that is not a heme ligand. It is reported here that such a well-defined example exists naturally in the membrane-anchored photosynthetic cytochrome *f*, a subunit of the cytochrome b_6f complex of oxygenic photosynthesis (*2*, *3*).

The narrow Soret (γ) and Q (α) bands of UV−visible redox difference spectra are spectral fingerprints of heme proteins. It has long been known that the visible spectrum of cytochrome *f* is different in chloroplasts and cyanobacteria (*4*, *5*). While the α band spectral peak occurs at 554 nm in the cytochrome b_6f complex or cytochrome *f* purified from chloroplasts [spinach (*6*), parsley (*7*), radish (*8*), turnip (*9*), charlock (*10*), and *Chlamydomonas reinhardtii* (*11*)], this maximum is red shifted to 556 nm in cyanobacteria [*Arthrospira maxima* (*5*), *Arthrospira flos-aquae* (*5*), *Synechocystis* sp. PCC 6803 (*12*), *Mastigocladus laminosus* (*13*), *Phormidium laminosum* (*14*), *Synechococcus* PCC 7002 (*15*), and *Anabaena variabilis* (*16*)]. In addition, the oxidation−reduction potential of the cyanobacterial cytochrome is significantly more reducing than that of the chloroplast cytochrome (*5*, *17*). An understanding of the structural basis for these differences in spectral and redox properties should be facilitated by comparison of the atomic structure of cytochrome *f* recently obtained from the cyanobacterium *P. laminosum* (*18*) with that from chloroplasts (*19*, *20*).

The atomic structure of turnip cytochrome *f* showed that the front face of the heme is shielded by N-terminal residues Tyr-1, Pro-2, Ile-3, and Phe-4, and also by Pro-117 and Pro-161 (*19*) (Figure 1). The Tyr-1 side chain, whose N-terminal α-amino group serves as an orthogonal heme ligand, is part of a hydrophobic heme environment that contributes to the very positive midpoint oxidation−reduction potential (E_{m7}[1] = 370 mV) of the chloroplast cytochrome *f* (*17*, *20*). The side chains of Tyr-1 and Pro-2 are nearly parallel to the heme

[†] These studies were supported by NIH Grant GM-18457 (W.A.C.), the Biotechnology and Biological Sciences Research Council and the Deutscher Akademischer Auslandsdienst (B.G.S.), and USDA Grant 98-35306-6405 (J.L.S. and W.A.C.).

* Corresponding author. Phone: (765) 494-4956. Fax: (765) 496-1189. E-mail: wac@bilbo.bio.purdue.edu.

[‡] Purdue University.

[§] University of Cambridge.

[1] Abbreviations: E_{m7}, midpoint oxidation−reduction potential at pH 7; MES, 2-(*N*-morpholino)ethanesulfonic acid; PCR, polymerase chain reaction; Phe, Trp, and Tyr, phenylalanine, tryptophan, and tyrosine, respectively.

10.1021/bi9928997 CCC: $19.00
Published on Web 04/29/2000

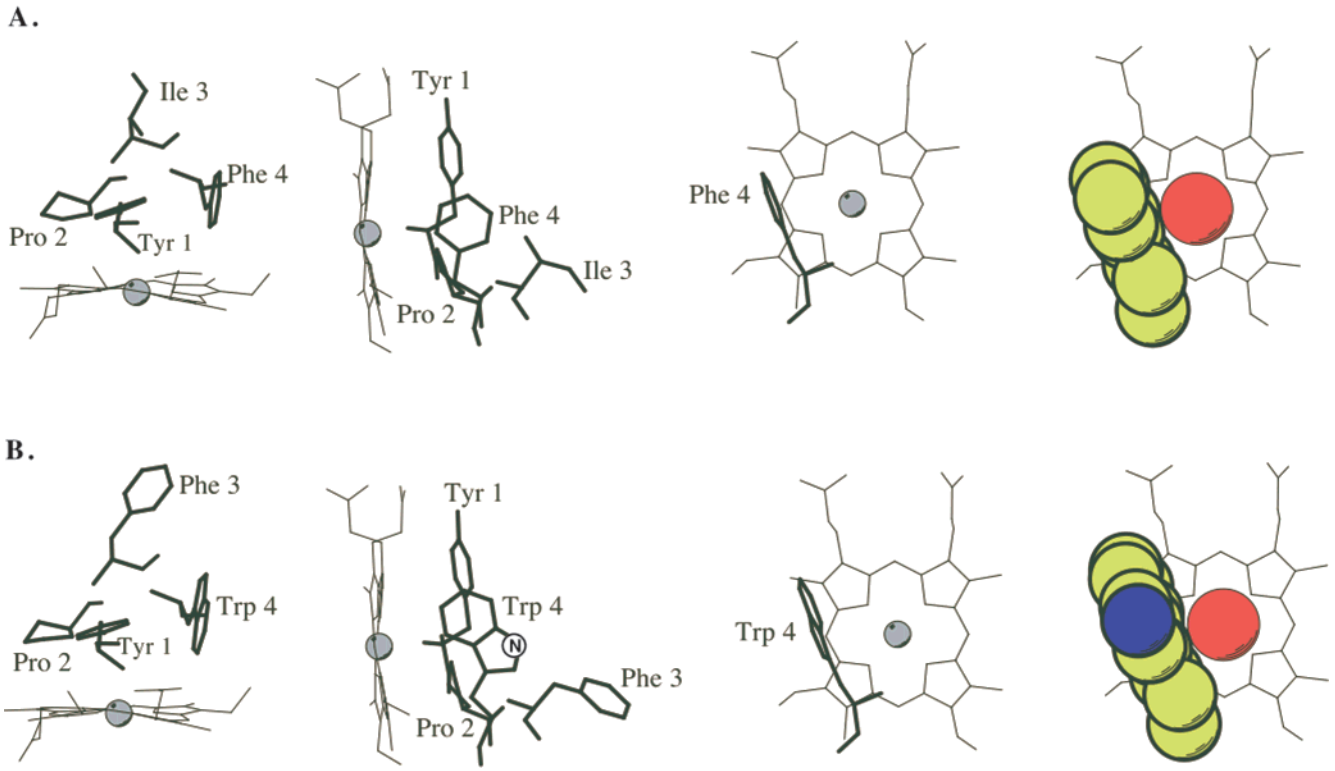

FIGURE 1: Orientation of the four N-terminal residues relative to the heme in the structure of cytochrome *f* from (A) turnip (*20*) and (B) *P. laminosum* (*18*). Three orthogonal views are shown in the first three panels. The orientation of the fourth panel is the same as that of the third. The closest approach of the aromatic ring of Trp (Trp $C_{\zeta 3}$ to heme C1D and C2D; Trp $C_{\epsilon 3}$ to heme CHD) or Phe (Phe $C_{\delta 2}$ to heme C4C or CHD) to the heme in the structures of cytochrome *f* from *P. laminosum*, turnip, and *C. reinhardtii* is 3.5−3.6 Å. The distance of closest approach of the Trp N atom to the heme plane is 7 Å. The angles between the planes created by the heme group and the aromatic side chain of residue 4 are 81°, 86°, and 83° in cytochrome *f* from *P. laminosum*, turnip, and *C. reinhardtii*, respectively. The larger Trp side chain extends over the tetrapyrrole 1.6 Å farther than the Phe side chain. The heme Fe is drawn as a shaded sphere in the first three panels. The carbon (yellow), nitrogen (blue), and iron (red) atoms are drawn with radii of 1.7 Å using the program MOLSCRIPT (*24*).

plane. Residue 1 is an aromatic residue (Tyr or Phe) in the 27 reported cytochrome *f* sequences (Table 1; *21*). Pro-2 is invariant in all sequences. The plant and algal sequences differ at positions 3 and 4 from six of the seven known cyanobacterial cytochrome *f* sequences (Table 1). Position 3 is always occupied by a hydrophobic residue. It is an aliphatic Ile or Val in all plant and algal sequences, and an aromatic Phe in almost all cyanobacterial sequences. From the atomic structures, the chloroplast Ile-3 and cyanobacterial Phe-3 face outward and do not contact the heme (Figure 1). Residue 4 contacts the heme and is always aromatic. It is Phe in almost all plant sequences, and Tyr in one plant sequence, *Marchantia polymorpha*, and in two algal sequences. However, residue 4 is Trp in six of the seven known cyanobacterial cytochromes (Table 1), for which the α band spectral peak is at 556 nm. It is of interest that residue 4 is Tyr in the seventh and last cyanobacterial cytochrome *f* sequence listed in Table 1, from *Synechococcus elongatus*, and that the α band peak of this cytochrome is at 554 nm (D. Schneider, P. Rich, and M. Rögner. personal communication), as it is in chloroplasts.

The distance, orientation, and extent of overlap of aromatic residue 4 with the heme determine the strength of their interaction. The nearest approach of the aromatic ring of Trp-4 or Phe-4 to the heme in the structures of cytochrome *f* from *P. laminosum* and turnip or *C. reinhardtii* is 3.5 Å, as seen in a wire model (Figure 1). The larger indole ring of the Trp side chain extends 1.6 Å farther over the heme tetrapyrrole and covers the methene bridge between the C and D pyrrole rings more completely than does the Phe side chain. The indole also partially occludes the D-pyrrole, which is not shielded by the Phe ring. The planes of the aromatic side chain of residue 4 and the heme are almost orthogonal, as the angle between them is 81° in *P. laminosum* (*17*), 86° in turnip (*19*), and 83° in *C. reinhardtii* (*23*).

MATERIALS AND METHODS

Mutagenesis. A PCR-based protocol was used to generate mutations in plasmid pUCPF2 (*11*) (*C. reinhardtii*) and plasmid pUC19li5 (*14*) (*P. laminosum*). Two mutagenic oligonucleotide primers, each complementary to opposite strands of the vector, were extended during PCR by means of *Pfu* DNA polymerase (Stratagene). The resulting PCR mixture was treated with the *Dpn*I restriction enzyme to digest the parental DNA template, selecting for the synthesized strand containing the mutation. MV1190 (*C. reinhardtii* cytochrome) or DH5α (*P. laminosum* cytochrome) *Escherichia coli* cells were transformed with the *Dpn*I-treated PCR mixture, and cells from antibiotic-resistant colonies were propagated. Plasmid DNA was analyzed by sequencing for the presence of the mutation and the intactness of the remainder of the gene.

Cytochrome f Expression. (A) C. reinhardtii Cytochrome. The culture conditions for expression of the 251-residue soluble truncated *C. reinhardtii* cytochrome *f* (intact cytochrome, 286 residues) in *E. coli* were as described previously (*11*, *25*). *(B) P. laminosum Cytochrome*. The mutated

Table 1: Alignment[a] of the First 26 or 27 Amino Acid Residues of Known Cytochrome *f* Sequences from (A) Higher Plants,[b] (B) Eukaryotic Algae,[c] and (C) Cyanobacteria[d]

Plants	
Turnip	YPI**F**AQQNYEN-PREATGRIVCANCHL...
Pea	YPI**F**AQQGYEN-PREATGRIVCANCHL...
Vicia faba	YPI**F**AQQGYEN-PREATGRIVCANCHL...
Soybean	YPI**F**AQQGYEN-PREATGRIVCANCHL...
Spinach	YPI**F**AQQGYEN-PREATGRIVCANCHL...
Tobacco	YPI**F**AQQGYEN-PREATGRIVCANCHL...
Oenothera	YPI**F**AQQGYEN-PREATGRIVCANCHL...
Corn	YPI**F**AQQGYEN-PREATGRIVCANCHL...
Rice	YPI**F**AQQGYEN-PREATGRIVCANCHL...
Wheat	YPI**F**AQQGYEN-PREATGRIVCANCHL...
Pine	YPI**F**AQQGYEN-PREATGRIVCANCHL...
Picea	YPI**F**AQQGYEN-PREATGRIVCANCHL...
Marchantia	FPI**Y**AQQGYEN-PREATGRIVCANCHL...
Maize	YPI**F**AQQGYEN-PREATGRIVCANCHL...
Algae	
Chlamydomonas	YPV**F**AQQNYAN-PREANGRIVCANCHL...
Porphyra	FPI**Y**AQQAYES-PREATGRIVCANCHL...
Cyanophora	FPI**Y**AQQAYQI-PREATGRIVCANCHL...
Odontella	YPV**F**AQQGYSN-PRAANGKLACANCHL...
Chlorella	YPI**F**AQQNYAN-PREANGRIVCANCHL...
Guillardia	FPV**F**AQQAYEN-PREATGRIVCANCHL...
Cyanobacteria	
Synechocystis	YPF**W**AQETAPLTPREATGRIVCANCHL...
Syn.PCC7002	YPF**W**AQQTAPETPREATGRIVCANCHL...
Nostoc	YPF**W**AQQTYPETPREPTGRIVCANCHL...
Arthrospira	YPF**W**AQETAPETPREATGRIVCANCHL...
Anabaena	YPF**W**AQQTYPETRPEPTGRIVCANCHL...
Phormidium	YPF**W**AQQNYAN-PREATGRIVCANCHL...
Syn.elongatus	YPF**Y**AQQGYES-PREATGRIVCANCHL...
	:* :**: ** *:: ******

[a] Invariant residues among 27 known cytochrome *f* sequences are marked with an asterisk and highly conserved residues with a colon. Sequences aligned with Clustal W (*22*). [b] Turnip, pea, *Vicia faba*, soybean, spinach, tobacco, *Oenothera hookerii*, corn, rice, wheat, pine, picea, *Marchantia polymorpha*, and maize. [c] *C. reinhardtii*, *Porphyra purpurea*, *Cy. paradoxa*, *Odontella sinensis*, *Chlorella vulgaris*, and *Guillardia theta*. [d] *Synechocystis* sp. 6803, *Synechococcus* PCC 7002, *Nostoc* sp., *Arthrospira maxima*, *Anabaena variabilis*, *P. laminosum*, and *Synechococcus elongatus*.

pUC19li5 plasmid was transformed into *E. coli* W3110 cells, and cytochrome *f* was expressed and purified as described previously (*14*).

Spectral Measurements. Difference spectra of *C. reinhardtii* and *P. laminosum* cytochrome *f* were measured in *E. coli* cell extracts in 25 mM phosphate buffer (pH 7.0) (*C. reinhardtii*) or 50 mM Tris (pH 7.5) and 100 mM NaCl (*P. laminosum*), using a Cary 3 or Perkin-Elmer Lambda 9 spectrophotometer, calibrated in each case to ±0.1 nm with the 656.1 nm emission line from an internal D_2 lamp. For the Q or α band, spectral values for absorbance maxima were obtained from reduced minus oxidized difference spectra; for the Soret band, they were obtained from absolute spectra of reduced (autoreduced from *E. coli* extracts) or oxidized proteins (ferricyanide was added to both sample and reference cuvettes at the same concentration). The different methods are necessitated by the absorbance of ferricyanide at 420 nm near the Soret band maximum. The α band spectra were fit well ($\chi^2 < 10^{-3}$, $r^2 = 0.998$) with two spectrally distinct components of the Voigt function, a combination of Lorentzian and Gaussian functions, using algorithms in PeakFit (Jandel Scientific).

Determination of the Cytochrome f Midpoint Potential. Midpoint oxidation−reduction potentials of the wild-type and mutant forms of cytochrome *f* were determined at pH 7.0 in 50 mM K_2HPO_4/KH_2PO_4 buffer while monitoring the absorbance at 554 nm. The initial potential (ca. 500 mV) was set by addition of 0.5 mM potassium ferricyanide and the titration carried out by subsequent addition of aliquots of sodium ascorbate to decrease the potential in 15−20 mV steps. The results were not changed by the use of the additional redox buffers: tetrachloro-*p*-benzoquinone (E_m = 340 mV), 2,5-dichloro-*p*-benzoquinone (E_m = 306 mV), 1,2-naphthoquinone-4-sulfonate (E_m = 210 mV), 1,2-naphthoquinone (E_m = 135 mV), and 1,4-naphthoquinone (E_m = 65 mV). The potential at each point of the titration was measured with a digital multimeter (Fluke 72 Series II or Philips PW9409). The electrochemical cell consisted of a Pt wire with an Ag/AgCl electrode in 1 M KCl (MF 2052 microelectrode, Bioanalytical Systems, or the Russell Type CMMPtRL electrode) as a reference (E_{ref} = 210−220 mV, or 221 mV in the *P. laminosum* cytochrome *f* titrations). The potential of the Ag/AgCl electrode was calibrated versus a saturated solution of quinhydrone (*26*). The titration was fit to a one-electron Nernst equation.

Stopped-Flow Kinetics of Cytochrome f Oxidation by Plastocyanin. The kinetics of cytochrome *f* oxidation by plastocyanin in solution were studied in 20 mM MES (pH 6.0), 0.1 M NaCl (*C. reinhardtii*), or 10 mM potassium phosphate (pH 6.0) and 90 mM NaCl (*P. laminosum*) using a stopped-flow spectrophotometer (Applied Photophysics model SX.18MV). The cytochrome *f* concentration was 0.1 μM, and that of plastocyanin was 15, 20, and 25 times greater so pseudo-first-order kinetics for the oxidation could be achieved. Oxidation was assessed by the decrease in the absorbance at the Soret band peak of the reduced cytochrome. The pseudo-first-order kinetic data were fit with a single exponential to obtain the first-order rate constant, k_{obs} (s^{-1}). The resulting k_{obs} values were plotted against the concentration of plastocyanin to obtain the bimolecular rate constant, k_2.

RESULTS

The Q or α band peak of algal *C. reinhardtii* wild-type cytochrome *f* is positioned at 554.1 ± 0.2 nm (Figure 2a). Of the nine mutant cytochromes that were examined (Table 2A), the only mutants with an α band red shift of ≥1 nm are those, F4W and V3F/F4W, that mimic the cyanobacterial cytochrome at residue 4 (Figure 2b). These mutant cytochromes *f* have α band peaks at 556.0 ± 0.2 and 556.2 ± 0.2 nm. Thus, the α band is red-shifted by 2.0 nm relative to that of the wild type in the mutants in which residue 4 is a Trp. These mutants also exhibit a pronounced "shoulder" at ~550 nm on the blue side of the α band (Figure 2b) that results in an asymmetric spectrum and a greater effective half-bandwidth. The α band of the low-spin cytochromes is among the sharpest spectral bands associated with protein-bound chromophores (bandwidth of cytochrome *f* at half-height = 9 nm) and can serve as a spectral fingerprint of heme-linked structure changes.

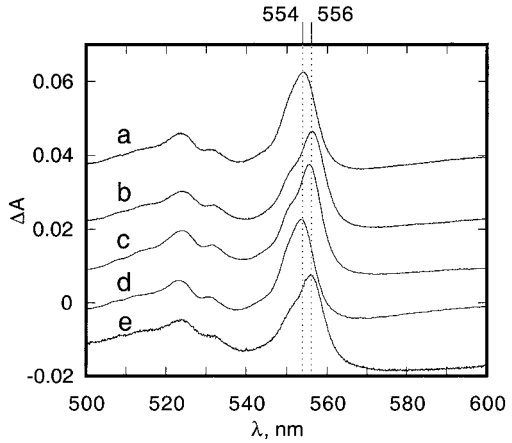

FIGURE 2: Q or α band chemical (ascorbate-ferricyanide) reduced minus oxidized spectra of cytochrome *f* from (a) the wild type of *C. reinhardtii*, (b) the F4W mutant of *C. reinhardtii*, (c) the wild type of *P. laminosum*, (d) the W4F mutant of *P. laminosum*, and (e) the *M. laminosus* cytochrome b_6f complex (*8*).

Table 2: Spectral Maxima of Chemical Difference Spectra (α band) and Absolute Spectra (Soret band) and Midpoint Potentials of the Wild Type and N-Terminal Mutants of *C. reinhardtii* and *P. laminosum* Cytochrome *f*

strain	α band λ_{max} (nm)	Soret band λ_{max} (nm) reduced	Soret band λ_{max} (nm) oxidized	E_{m7} (mV)[a]
		(A) *C. reinhardtii*		
wild type	554.1 ± 0.2	421.1 ± 0.2	410.0 ± 0.4	370 ± 3
Y1F	554.6 ± 0.2	421.8 ± 0.2	411.0 ± 0.4	369 ± 3
Y1S	552.9 ± 0.2	420.2 ± 0.2	409.0 ± 0.4	313 ± 7
P2V	554.0 ± 0.2	420.1 ± 0.2	409.7 ± 0.4	241 ± 7
V3F	554.3 ± 0.2	421.3 ± 0.2	410.1 ± 0.4	373 ± 4
F4L	553.7 ± 0.2	420.5 ± 0.2	409.7 ± 0.4	348 ± 7
F4W	556.0 ± 0.2	422.0 ± 0.2	410.4 ± 0.2	336 ± 3
Y1F/F4Y	554.6 ± 0.2	421.8 ± 0.2	411.0 ± 0.4	370 ± 4
Y1S/F4L	552.8 ± 0.2	419.5 ± 0.2	409.0 ± 0.4	289 ± 5
V3F/F4W	556.2 ± 0.2	422.1 ± 0.2	410.5 ± 0.4	342 ± 5
		(B) *P. laminosum*		
wild type	555.7 ± 0.2	421.6 ± 0.2	410.5 ± 0.2	297 ± 4
W4F	553.7 ± 0.2	420.7 ± 0.2	410.2 ± 0.2	323 ± 4
W4L	553.6 ± 0.2	419.8 ± 0.2	410.0 ± 0.2	300 ± 4
F3V/W4F	553.7 ± 0.2	420.5 ± 0.2	410.0 ± 0.2	316 ± 2
		(C) *Ma. laminosus*		
wild type	556.0 ± 0.2	nd	nd	326 ± 3[b]

[a] Midpoint redox potential at pH 7; nd, not determined. [b] Measured in the b_6f complex.

In the cyanobacterium *P. laminosum*, the 555.7 nm α band difference peak of the wild-type cytochrome (Figure 2c) is blue-shifted by 2.0 nm when Trp-4 is replaced with Phe (Figure 2d), which mimics the algal cytochrome, or with Leu (Table 2B). There is no additional spectral shift if residue 3 (Phe) is also changed to mimic the algal cytochrome (Val). A pronounced "shoulder" at 550 nm becomes apparent when residue 4 is Trp, as in mutants of the algal cytochrome or in the cyanobacterial wild type. This arises from the increased degree of wavelength separation between the major α band peak and the low-amplitude shoulder, as quantitated by deconvolution of the spectra.

The 2 nm shift of α band peak values corresponds to an energy (wavenumber) shift of 64 cm^{-1}, a relatively small energy shift equivalent to 0.18 kcal/mol. A similar energy shift of 50 cm^{-1} was found for the wavelength shifts of the Soret band of cytochromes in which Phe and Trp were exchanged at position 4. The Soret band in the *C. reinhardtii* F4W and *P. laminosum* W4F mutant cytochromes *f* is shifted in the same direction as the α band (Table 2A,B). The Soret band peak of the reduced proteins, at 421.1 and 421.6 nm in the wild type of *C. reinhardtii* and *P. laminosum*, respectively, is red-shifted by 0.9 nm to 422.0 nm in the *C. reinhardtii* F4W mutant (Table 2A) and blue-shifted by 0.9 nm to 420.7 nm in the *P. laminosum* W4F mutant (Table 2B), a wavenumber shift of 50 cm^{-1}. An additional 0.2 nm shift in the Soret band, close to the limit of our experimental accuracy, would make its energy shift the same as in the α band. The similarity of the energy shifts in the α and Soret bands suggests that the spectral shifts may have a common origin.

Several mutations at other positions in the N-terminal heme shielding peptide cause a blue shift in the α and Soret bands. However, a significant red shift associated with changes of these residues was not observed. Substitution of the N-terminal Tyr-1 in the *C. reinhardtii* cytochrome in the mutant Y1S (*27*) resulted in 1.2 and 0.9 nm blue shifts in the α and Soret bands, respectively (Table 2A). These spectral shifts were accompanied by a decrease of 55−60 mV in the redox potential (Table 2A), which is attributed to an increase in the extent of exposure of the heme to the bulk aqueous phase (*1*, *28*, *29*). When these two mutational changes were combined in the double mutant Y1S/F4L, the spectral blue shift in the Soret band was slightly increased, and that in the α band was no greater than in either of the single mutants. The negative shift in the E_{m7} value of the double mutant (−81 mV) is close to the sum of the shifts (−79 mV) in the single mutants. Substitution of Phe-4 in the *C. reinhardtii* cytochrome *f* with a hydrophobic residue, Leu, caused no red shift in either the α or Soret bands (Table 2A).

There are four known cytochrome *f* sequences (*M. polymorpha*, *Porphyra purpurea*, *Cyanophora paradoxa*, and *Guillardia theta*), for which residue 1 is Phe instead of Tyr, in the first three of which residue 4 is Tyr instead of Phe. The effect of these substitutions of aromatic residues was studied through mutants Y1F and F4Y of the *C. reinhardtii* cytochrome *f*. The F4Y mutation did not affect the spectral or redox properties of cytochrome *f*, whereas the Y1F mutation caused a small red shift of the α (0.5 nm) and Soret (0.7 nm) bands and had no effect on the E_m (Table 2A).

The midpoint oxidation−reduction potential (E_{m7}) is significantly less positive (297 mV) in the cyanobacterial *P. laminosum* cytochrome *f* compared to the midpoint potential (370 mV) of the chloroplast cytochrome (Table 2A,B). The less positive, more reducing potential is characteristic of the cyanobacterial cytochromes, as the E_{m7} is 326 mV for cytochrome *f* in the cytochrome b_6f complex from the thermophilic cyanobacterium, *Ma. laminosus* (*13*). The E_{m7} values of the reciprocally altered F4W and W4F mutant proteins, from *C. reinhardtii* and *P. laminosum*, are shifted by −34 and 26 mV, respectively. This shift is 40−50% of the 70 mV difference between the *C. reinhardtii* and *P. laminosum* wild-type cytochromes (Table 2A,B).

DISCUSSION

Basis for Spectral Shifts. The dependence of the heme α and Soret bands shifts on the identity of the aromatic residue at position 4 implies that the energy of both the $a_{1u} \rightarrow e_g$

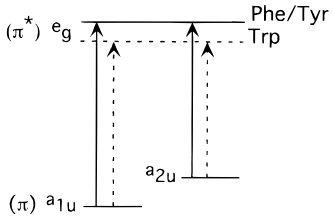

FIGURE 3: Energy level diagram for Soret and α band optical transitions $a_{1u} \rightarrow e_g$ and $a_{2u} \rightarrow e_g$ (*30*), respectively, of low-spin heme proteins. The dashed line shows schematically that the optical transition energies are smaller (dashed) in cytochrome *f* when residue 4 is Trp compared to when it is Phe or Tyr. The π^* excited state of cytochrome *f* with Trp-4 is shown to have an energy that is lower than that of the cytochrome with Phe-4 or Tyr-4, as discussed in the text.

Soret and $a_{2u} \rightarrow e_g$ α band transitions decreases by approximately 60 cm^{-1} in the Trp-4 cytochromes compared to the Phe-4 cytochromes. This could arise from a decrease in the energy of the excited π^* e_g state of the heme in the Trp-4 cytochrome, as shown in Figure 3, and/or an increase (not shown) in the energy levels of the ground state π a_{1u} and a_{2u} orbitals. Arguments for the energy level scheme shown in Figure 3 are as follows. (a) A shift of the single excited state energy level of the heme would account for the shift of both Soret and α bands, and (b) the more delocalized π^* state orbitals, which extend farther toward the heme periphery, may interact more strongly with the π or σ orbitals of residue 4 and may be more sensitive to residue changes at this position (Figure 1A vs Figure 1B, right panel). Pairwise $\pi-\pi$ interaction energies of aromatic molecules have been calculated as a function of the angular orientation and lateral offset of two aromatic systems (*31*). In the "edge-on" configuration geometry that describes the interactions of the residue at position 4 with the heme (Figure 1), an attractive π (heme)$-\sigma$ (aromatic residue) system should dominate these interactions (*31*). The differential effect on the optical transitions could then be explained as a lowering of the energy of the π^* excited state (Figure 3) because of a stronger attractive interaction of the heme π^* system with Trp. The decreased midpoint potential in the presence of Trp-4 is most readily explained (see below) in terms of a greater electrostatic repulsive interaction of the Trp π system (*31*, *32*) with the heme Fe orbitals.

In principle, Tyr, because of its ability to ionize, need not behave like Phe. However, no difference between these two aromatic residues was found in the work presented here. It is likely that the effective p*K* of the Tyr (ca. 10) is too high to allow ionization in measurements made at pH 7−7.5. A special role for the indole nitrogen and an N-based Trp dipole are precluded by an orientation of the indole with the nitrogen atom pointing away from the heme (Figure 1B, second panel) and the large distance (7 Å) of the N atom of the Trp from the heme plane.

Basis for Redox Potential Shifts. The changes in redox potential between the wild type and the residue 4 mutant of cytochrome *f* from *C. reinhardtii* and *P. laminosum* cannot readily be explained in terms of changes in solvent accessibility (*1*, *28*, *29*), since the more negative potential is associated with the better shielding Trp. It is proposed that the π-based repulsive negative electrostatic interaction of aromatic residue 4 with the heme Fe orbitals preferentially stabilizes the oxidized form of the cytochrome. Hence, the stronger influence of the Trp indole ring, compared with that of Phe, should cause a less positive midpoint redox potential, as observed in the F4W mutant of *C. reinhardtii*, and the converse in the W4F mutant of *P. laminosum*. When residue 4 is Leu, a greater stabilization of the reduced form would be expected because of the smaller electrostatic interaction. In fact, the opposite is observed, with the Leu-4 mutant having an E_{m7} value that is closer to the less positive value of the Trp-4 cytochrome. From examination of differential solvent accessibilities of the heme in the N-terminal mutants compared to those in the wild type, carried out as described in ref *29*, the decreased potential of the Leu-4 compared to the Phe-4 proteins, as well as of Y1S in *C. reinhardtii* (Table 2), is probably due to increased solvent accessibility of the heme (calculations not shown). The calculations of accessibility are only semiquantitative because they are dependent on an empirical correlation which is subject to a large margin of error, and the heme accessibility in the wild type is small (*29*).

Functional Significance of Residue 4. A role of residue 4 in the electron transfer or docking reaction of cytochrome *f* with its electron acceptor, plastocyanin, is indicated by a decreased second-order rate constant for electron transfer to plastocyanin in the Phe-4 cytochrome *f* relative to that with the Trp-4 cytochrome. The decrease was 2.7-fold, from 4.4 $\times$ 10^7 M^{-1} s^{-1} for the wild type to 1.7 $\times$ 10^7 M^{-1} s^{-1} for the W4F mutant of *P. laminosum*, using *P. laminosum* plastocyanin (data not shown). Conversely, the rate constant increased 1.5-fold, from 2.1 $\times$ 10^8 in the *C. reinhardtii* wild type to 3.2 $\times$ 10^8 M^{-1} s^{-1} in the F4W mutant. Straightforward application of electron transfer theory predicts that the changes of E_{m7} in the mutants of cytochrome *f* (Table 2) could account for 1.6−1.8-fold changes in the cytochrome *f* $\rightarrow$ plastocyanin electron transfer rate (*33*). The question of whether the 2.7-fold decrease in the rate constant found in the W4F mutant is significant requires further investigation.

In conclusion, one expects that the combination of the increased availability of sequence data, together with high-resolution structures and spectra, should allow for an improved understanding of the basis for observed variations in spectral and redox properties of redox-active proteins, including cytochromes. In the case presented here, the specific effect of residue 4 on the visible spectrum and redox potential of cytochrome *f* introduces a novel effect of structure on cytochrome spectra, as well as on the redox properties associated with the function of the cytochrome.

ACKNOWLEDGMENT

We are indebted to G. M. Soriano for experimental collaboration and advice, to G. T. Babcock, H. B. Gray, G. Mauk, D. R. McMillin, J. Wilker, and W. H. Woodruff for helpful discussions, and to Carol Greski for expert assistance with the manuscript.

REFERENCES

1. Moore, G. R., and Pettigrew, G. W. (1990) *Cytochromes c*, pp 255−307, Springer-Verlag, New York.
2. Cramer, W. A., Soriano, G. M., Ponamarev, M., Huang, D., Zhang, H., Martinez, S., and Smith, J. L. (1996) *Annu. Rev. Plant Physiol. 47*, 477−508.
3. Kallas, T. (1994) in *The Molecular Biology of Cyanobacteria* (Bryant, D. A., Ed.) pp 259−317, Kluwer Academic Publishers, Dordrecht, The Netherlands.

4. Cramer, W. A., and Whitmarsh, J. (1977) *Annu. Rev. Plant Physiol. 28*, 133−172.
5. Ho, K. K., and Krogmann, D. W. (1980) *J. Biol. Chem. 255*, 3855−3861.
6. Singh, J., and Wasserman, A. R. (1971) *J. Biol. Chem. 246*, 3532−3541.
7. Forti, G., Bertole, M. L., and Zanetti, G. (1965) *Biochim. Biophys. Acta 109*, 33−40.
8. Takahashi, M., and Asada, K. (1975) *Plant Cell Physiol. 16*, 191−194.
9. Szczepaniak, A., Huang, D., and Cramer, W. A. Unpublished data.
10. Gray, J. C. (1978) *Eur. J. Biochem. 82*, 133−141.
11. Ponamarev, M. V., and Cramer, W. A. (1998) *Biochemistry 37*, 17199−17208.
12. Zhang, L., Pakrasi, H. B., and Whitmarsh, J. (1994) *J. Biol. Chem. 269*, 5036−5042.
13. Huang, D., Soriano, G. M., and Cramer, W. A. Unpublished data.
14. Schlarb, B. G., Wagner, M. J., Vijgenboom, E., Ubbink, M., Bendall, D. S., and Howe, C. J. (1999) *Gene 234*, 275−283.
15. Kallas, T. Personal communication.
16. Krinner, M., Hauska, G., Hurt, E., and Lockau, W. (1982) *Biochim. Biophys. Acta 681*, 110−114.
17. Davenport, H. E., and Hill, R. (1952) *Proc. R. Soc. London, Ser. B 139*, 327−345.
18. Carrell, C. J., Schlarb, B. G., Bendall, D. S., Howe, C. J., Cramer, W. A., and Smith, J. L. (1999) *Biochemistry 38*, 9590−9599.
19. Martinez, S. E., Huang, D., Szczepaniak, A., Cramer, W. A., and Smith, J. L. (1994) *Structure 2*, 95−105.
20. Martinez, S., Huang, D., Ponomarev, M., Cramer, W. A., and Smith, J. L. (1996) *Protein Sci. 5*, 1081−1092.
21. Sequences for plant, algal, and cyanobacterial cytochromes *f* were obtained from GenBank.
22. Thompson, J. D., Higgins, D. G., and Gibson, T. J. (1994) CLUSTAL W, *Nucleic Acids Res. 22*, 4673−4680.
23. Sainz, G., Carrell, C. J., Ponamarev, M. V., Soriano, G. M., Cramer, W. A., and Smith, J. L. (2000) *Biochemistry* (submitted).
24. Kraulis, P. J. (1991) *J. Appl. Crystallogr. 24*, 946−950.
25. Thöny-Meyer, L., Fischer, F., Kunzler, P., Ritz, D., and Hennecke, H. (1995) *J. Bacteriol. 177*, 4321−4326.
26. Clark, W. M. (1960) *Oxidation-reduction potentials of organic systems*, pp 584, Williams and Wilkins, Baltimore.
27. Zhou, J., Fernandez-Velasco, J., and Malkin, R. (1996) *J. Biol. Chem. 271*, 6225−6232.
28. Schlauder, G. G., and Kassner, R. J. (1979) *J. Biol. Chem. 254*, 4110−4113.
29. Tezcan, F. A., Winkler, J. R., and Gray, H. B. (1998) *J. Am. Chem. Soc. 120*, 13383−13388.
30. Gouterman, M. (1978) in *The Porphyrins* (Dolphin, D., Ed.) Vol. 3, pp 1−156, Academic Press, New York.
31. Hunter, C. A., and Sanders, J. K. M. (1990) *J. Am. Chem. Soc. 112*, 5525−5534.
32. Dougherty, D. A. (1996) *Science 271*, 163−167.
33. Marcus, R., and Sutin, N. (1985) *Biochim. Biophys. Acta 811*, 265−322.

BI9928997